Special Issue: Vesuvius monitoring and knowledge

19 years of tilt data on Mt. Vesuvius: state of the art and future perspectives

Ciro Ricco*, Ida Aquino, Sven Ettore P. Borgstrom, Carlo Del Gaudio

Istituto Nazionale di Geofisica e Vulcanologia, Sezione di Napoli, Osservatorio Vesuviano, Naples, Italy

Article history
Received August 3, 2012; accepted July 8, 2013.
Subject classification:
Monitoring, Tilt network, Ground deformation, Vesuvius.

ABSTRACT

Mt. Vesuvius, located along the SW border of the Campania Plane graben, is one of the most studied volcanoes worldwide, from both the volcanological and the geophysical, geochemical and geodetic point of view. In order to better understand its dynamics, the deformation of the volcano has been already studied since the early '70s by setting up levelling lines and, since a few years later, through trilateration networks, whereas ground tilt monitoring started in 1993. Tilt variations were recorded by an automatic surface station set up at the Osservatorio Vesuviano (O.V.) bunker (OVO) and data recorded were transmitted to the O.V. Surveillance Centre in Naples. Afterwards, in 1996 two more identical stations were set up close to Torre del Greco (CMD), and close to Trecase (TRC). In 2002 the data acquisition system was replaced, while at the end of 2011 a Lily borehole sensor was set up at 26 m depth, replacing the old TRC tilt station. The paper describes in details the tilt network of Mt. Vesuvius, its development over time and the data processing procedure; moreover, the ground deformation pattern is discussed, as inferred from the study of 19 years of data and its change during the seismic crises of 1995-1996 and 1999-2000. From the information obtained from the tiltmetric monitoring, a complex deformation pattern can be deduced, strongly dependent on the position of the sites in which the sensors were set up with respect to the morphology of the volcanic edifice and its structural outlines. If we consider the signals as they were recorded, although previously corrected for the influences of the thermo-elastic strain on the sensors, the tilting occurs mainly in the SW direction with rates of about 11 μradians/year on both the western and eastern flanks and of about 13 μradians/year on the southern one. Because tilt vectors point in the long term outward from the summit and towards the subsiding area, this supports the hypothesis of a southern areas subsidence, according with a spreading effect of Vesuvius, taking into account geological, structural, geophysical and geodetical (optical levelling, InSAR) data. The SW tilting occurs therefore irregularly and shows some seasonalities, consistent with the solar thermal radiation whose removal by statistical procedure outlines a different but equally interesting deformation field as it shows interruptions with changes in both trend and amplitude during two periods of strong seismic activity that affected Mt. Vesuvius in the periods 1995-1996 and late 1999-2000, marked by an average rate of energy release of at least one order of magnitude greater than the previous and following periods. Another change in intensity and direction of the deformation detected by tiltmeters since 2000, connected with the variations of the phase shift between the tilt components and the temperature recorded, compared to previous years, occurs during a strong decrease of the energy released by Vesuvius earthquakes.

1. Volcanological setting and geodynamic context

The Somma-Vesuvius volcanic complex together with the volcanic fields of Campi Flegrei, Ischia Island and Procida Island (Figure 1), is part of the alkali-potassic volcanic province of Central Italy and formed at the intersection of two regional fault systems with stress directions NW-SE and NE-SW [Ippolito et al. 1973, Pescatore and Sgrosso 1973].

Vesuvio is located in the southern sector of the Campania Plain, a Plio-Quaternary structural depression extending from the western part of the Apennine chain to the eastern coast of the Tyrrhenian Sea [Aprile and Ortolani 1979, Scandone 1979, Doglioni 1991].

The Somma-Vesuvius volcanic complex consists of the relatively old strato-volcano, Mount Somma that underwent a series of caldera collapses culminating 18 ky B.P. [Cioni et al. 1999] and the younger intracaldera cone of Vesuvius.

Vesuvius is characterised by a great variability in eruptive style: highly explosive, subplinian and plinian eruptions alternating with periods of effusive eruptions consisting in relatively frequent open-conduit activity sometimes accompanied by Strombolian events that typically followed long periods of quiescence [Arnò et al. 1987, Santacroce 1987, Rolandi et al. 1998, Arrighi et al. 2001].

After the last subplinian eruption, taking place in 1631 [Rosi et al. 1993], Vesuvius was marked by open-conduit activity, which ended with the eruption of 1944. The alternating activity of Vesuvius resulted in

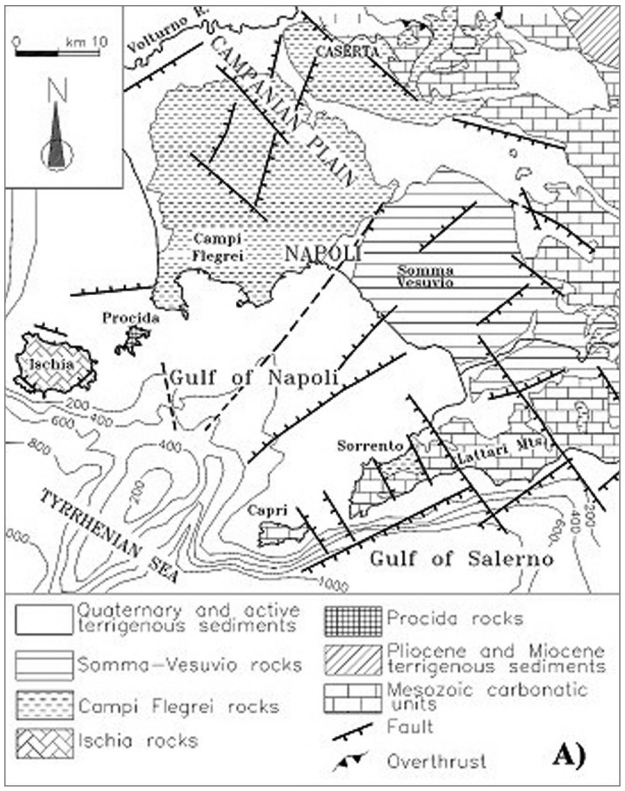

Figure 1. Geological sketch map of the Campanian sector of the Appenine Chain showing location of both Campanian Plain and Campanian volcanic districts (modified after Santacroce [1987]).

different deposits including pyroclastic products (scoriae, pumice, lapilli) and products such as compact lavas and cinders.

As regard to the Vesuvius dynamics, from the joint analysis of InSAR (SBAS approach) [Berardino et al. 2002] and optical levelling data, Lanari et al. [2002] highlight a subsidence located in two different areas of the volcano: the central cone and a semicircular narrow strip around the volcanic edifice, although discontinuous, 9-10 km away from the crater within the Campania Plain graben, located W, N and E of the volcano. Both areas are marked by a nearly continuous subsidence in the time span investigated by the Authors (1992-2000), with different deformation rates ranging from 0.3 to 0.8 cm/year and an overall subsidence of 5-7 cm.

Subsidence can be interpreted for both sites considering joint effects of gravitational sliding and extensional tectonic stress occurring at the contact between different lithological units; for the central cone, the contact occurs between the younger Vesuvius rocks and Mt. Somma older ones, whereas in the semicircular strip the contact is between volcanic rocks and the sedimentary basin.

Afterwards, Borgia et al. [2005] interpret the subsidence as related to a spreading effect of Vesuvius, taking into account geological, structural, geophysical and geodetical (optical levelling, InSAR) data. They assert that Vesuvius began to spread onto its sedimentary basin about 3,600 years B.P. at a rate of a few mm/year and it will be spreading for additional 7,200 years, based on specific modeling.

The spreading, which appears as an extension of the summit part of the crater coupled with a basal compression, according to the Authors resulted in a decrease in time of the VEI (*Volcanic Explosivity Index*) therefore suggesting that Plinian eruptions at Vesuvius are less likely to occur in the near future whereas fissure eruptions, preceded by moderate explosive phases, appear to be a more probable scenario.

Moreover, Borgia et al. [2005] exploit SAR Interferometry to infer a detailed structural sketch of the whole Vesuvius area, taking into account data from both ascending and descending orbits. This has allowed, for common pixels seen by the two viewing geometries, to split ground motion in a vertical component (vertical mean deformation velocity map), afterwards successfully compared with optical levelling data and in a E-W component (E-W mean deformation velocity map).

From the analysis of the maps the Authors point out, besides the subsidence effects of the semicircular strip around the volcanic edifice (> 2 mm/year) and the summit part of the crater, as mentioned before:

– a regional scale subsidence, with the SE sector of the image subsiding 1-2 mm/year with respect to the NW one, also moving eastwards;

– the relative uplift of the Pompei area (1-2 mm/year).

2. Importance of tilt monitoring and previous measurements

All those phenomena related to chemical and physical variations in a volcanic apparatus referable to overpressure in a magma chamber could take on a large interest because they often are the precursors of eruptions. Their identification and time evolution during the volcano quiescence are one of the most important goals for hazard mitigation based on seismic, geochemical and geodetic monitoring techniques.

In particular, volcano geodesy studies the variations in shape of the volcano edifice caused by magma uprising; among the geodetic techniques applied to an active volcanic area, the tiltmetry is able to detect the tilt variations in direction and amplitude.

Tilt measurements are very important because it is known that, during an inflation episode, the flanks of volcanoes deform reaching variations of inclination in the order of ten microradians; jointly with other geodetic methods, they are a valuable technique for monitoring the time evolution of volcanic deformation, recording the angular component of strain. Tilt arrays currently operate in many active volcanoes of the world, besides at Vesuvius, in Phlegraean Fields, Etna and Aeo-

lian Islands [Ricco et al. 2003, Gambino et al. 2007, Genco et al. 2010, Ferro et al. 2011], on other volcanos as Kilauea (Hawaii), Krafla (Island), Piton de la Fournaise (Indian Ocean), Galeras and Nevado del Ruiz (Colombia), Tacanà e Fuego (Mexico-Guatemala), Mayon e Taal (Filippines), Merapi and Soputan (Indonesia), Unzen (Japan) [Dzurisin 1992].

Tilt monitoring is carried out at Vesuvius in order to control volcano movements, checking the smallest variations of ground inclination.

From bibliography [Imbò 1939], we know that already in 1935 the first successful clinometric measurements were made by G. Imbò (O.V. director) on the Vesuvius. In 1935 he installed the spirit levels on the seismic pillar of the O.V. historical building and measured, by recording on smoked paper, the apparent deviation of the vertical from October 1935 to January 1939, highlighting a direct correlation between the SSW apparent tilt of the volcano and a lowering of the eruptive column, during a phase of activity on the crater bottom, and NNE tilt and the uplifting of the column [Imbò 1939].

In order to better understand its dynamics, the deformation of the volcano has been studied since the early '70s by setting up levelling lines and, starting from a few years later, through trilateration networks.

3. Tilt network, localization and technical features

Ground tilt monitoring started in 1993, with the installation of a tilt station in the gallery of the historical Site of the O.V. at Ercolano (OVO station), followed in 1996 by two more stations respectively located at Torre del Greco, Camaldoli site (CMD station) and at Trecase, in the Forest Station (TRC station; Aquino et al. [2006]) (Figure 2).

Indeed, the first station (OVO) was set up on February 1992 but it started working from 1993; it was equipped with a surface tiltmeter with data sampling of 6 samples per hour with 12 bit acquisition and telephone wire transmission.

On November 2002 the acquisition control unit was replaced, reprogramming data sampling to 12 samples per hour with storage on datalogger and data transmission to the O.V.

The bunker inside the Historical Site of the O.V. was chosen for the installation, 35 meters deep from the surface, at 608 m a.s.l. and 2.5 km from the crater, in WNW direction; this station is still working.

The CMD station was installed on June 1996, equipped and configured as the OVO station; on September 2003 the acquisition control unit was replaced, reprogramming data acquisition and transmission to the O.V. as the OVO station.

The instrumentation was located on a hillock close

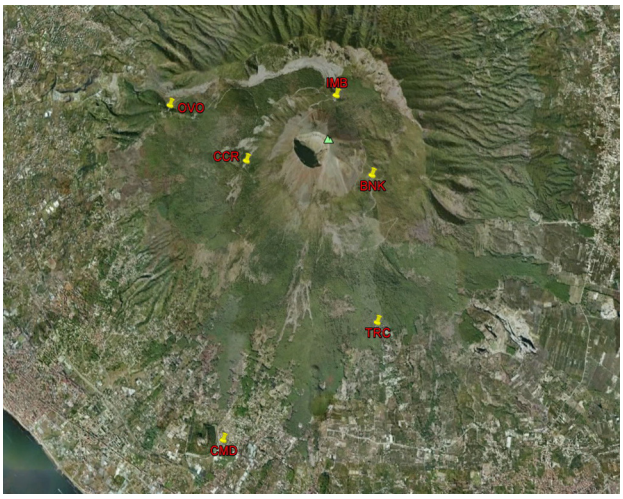

Figure 2. Tilt network for ground monitoring at Mt. Vesuvius; at CCR, IMB and BNK sites was drilled a well at a depth ranging from 20 to 26 meters that will be instrumented within 2012.

to the vesuvius aqueduct in Cupa dei Camaldoli (Torre del Greco) site in a well two meters deep from the surface at 120 m a.s.l., 5 km from the crater in SSW direction; besides tilt and thermal data, this station acquired also the atmospheric pressure. This station is presently working as well.

The last station (TRC) was set up on March 1996, equipped and configured as OVO and CMD stations; on November 2002 the acquisition control unit was replaced, reprogramming data acquisition and transmission to the O.V. as the OVO and CMD stations.

The instrumentation was located close to the Trecase Forest Station inside a basement at the surface level, at 370 m a.s.l. and 2.9 km from the crater in SSE direction; this station was removed on November 2007 for renovation of the hosting site.

All stations are equipped with sensors model AGI 702 (bi-axial, bubbletype, manufactured by Applied Geomechanics); tilt variations are measured along 2 orthogonal directions X and Y aligned to West-East and North-South axes. The sensors have a dynamic range of ± 800 μrad in high gain, a resolution of 0.1 μrad and a sensitivity of 10 mV/μrad; they are also equipped with a temperature sensor with resolution of 0.1 °C [AGI 1988].

Data acquisition system is the HANDI-LOGGER model 798-A of Geomechanics, equipped with a datalogger CR10X collecting and storing the data from tiltmeters at a sample rate of 12 samples per hour. The station also acquires the supply voltage [AGI 2001] before the telematic connection with O.V. Surveillance Centre in Naples.

4. Tilt network renovation with borehole sensors

It is known that bubble-tiltmeters are very sensitive to temperature variations; as during the day the solar radiation heats the ground, the thermal variations cause

a first order effect on the surface tiltmeters, mainly if the medium is heterogeneous [Harrison and Herbst 1977]. This effect is proportional to the thermal dilatation of the invar screws mounted at the base of the sensor; these screws have to be therefore of the same length. Even the electrolytic transducer is subject to thermal fluctuations since the liquid is subjected to contraction and expansion with the consequent change of the scale factor *SF*cal (angular coefficient of the calibration line). If we do not take into account these effects due to the difference between the environmental temperature (*Te*) and the calibration temperature (*T*cal), the measured tilt angle will be different from the real one. The thermal compensation is calculated through the two correction coefficients K_s and K_z experimentally measured in the laboratory. The compensation of the tilt signal due to *Te* does not correct the thermo-elastic deformation, which is greater on the surface. This effect is present in the signals recorded by surface tiltmeters and may hide the ground tilt linked to volcanic activity, thereby modifying the spectral content of the signals. In order to dampen the thermal excursions, the surface sensors are generally installed in caves.

It's therefore preferable to install the tilt sensors at depth, where thermal oscillations are minimum; for this reason it was decided to use the borehole tiltmeters [Wyatt et al. 1988, Jentzsch et al. 1993, Zadro and Braitenberg 1999].

The project of tilt network renovation at Mt. Vesuvius involves four new borehole stations and therefore corresponding wells were drilled between 2010 and 2012 at depths ranging from 20 to 26 meters, respectively named CCR (760 m a.s.l., 1.2 km from the crater in WSW direction), IMB (970 m a.s.l., 0.9 km from the crater in NNE direction), BNK (870 m a.s.l., 1.2 km from the crater in ESE direction) and TRC (same place of the old station closed in November 2007) (Figure 2).

The wells were realized with a CMV hydraulic crawler drill MK 600 M, 76 mm pipes, 101 mm core drills and 127 mm casings, with drilling muds prepared with a water-polymers mixture; as the wells were completed, they were isolated at the bottom with a cement plug and coated with 80 mm PVC pipes.

The first three wells have been instrumented within 2012 while the last one was equipped at the end of November 2011 with a tiltmeter located 26 m deep.

This tiltmeter was a LILY model (Self-Levelling Borehole Tiltmeter) from the Applied Geomechanics, made with a self-levelling sensor on a range of ± 10 degrees, with a dynamic range of ± 330 μradians and a resolution less than 5 nanoradians; this is stainless steel with a cylindrical shape and inside its bottom the electrolytic bubbles, the thermal sensor, the magnetic compass (for detecting the change of magnetic declination in terms of counterclockwise azimuth from N), the self-levelling device and the electronics are located. Data digitally acquired are transmitted to the surface with a RS232 protocol on wires with a length less than 15 meters or RS485. Each data string contains the X and Y components directly in radians, the magnetic azimuth in degrees, the temperature in °C, the date and the hour, minutes, seconds, the power supply in mV and the sensor serial number [AGI 2005].

To lower the sensor into the hole in order to get the tilt plane of the Y component aligned with the magnetic N, a battery of rods two meters each one was specifically designed; the rods were built in anodized aluminium with a rectangular section, specifically conceived to be jointly attached to each other. The tiltmeter was therefore fixed to the first rod through an electric lock electronically controlled for the sensor release once it reached the bottom of the hole; afterwards it was covered by fine quartz sand. Once the installation was completed the sensor self-levelling procedure started for data storage on the sensor local memory besides their periodic transfer to a dedicated computer.

Currently the sampling rate is 60 samples per hour and each acquisition is the mean value of 8,000 samples; data download is currently carried out locally as we are waiting for the activation of the power supply and the wireless network that will allow automatic data download.

5. Data processing

Tilt signals recorded from 1993 till now represent a valuable information on the deformation that affects in the last 19 years the flanks of Mt. Vesuvius. As we are dealing with surface sensors, as already mentioned, the tilt recorded, besides containing information on the volcano dynamics, is mostly due to expansion/contraction of the rocks subject to thermal variations that is hard to model due to the variability in the subsurface of the thermal expansion coefficient [Braitenberg 1999, Grillo et al. 2011, Tenze et al. 2012]. The signals are disturbed also by rainfalls, height variations of the sea-level, strong atmospheric perturbations, atmospheric pressure, ocean loading and earth tides [Harrison 1976, Braitenberg et al. 2001, Westerhaus and Welle 2002].

For each station of the tilt network, four data-series are available; the first two are the S-N and W-E components, the third one concerns air temperature at the soil level and the last one is the supply voltage.

The W-E and S-N components are combined into a vectorial plot of the tilt variation over time. Every

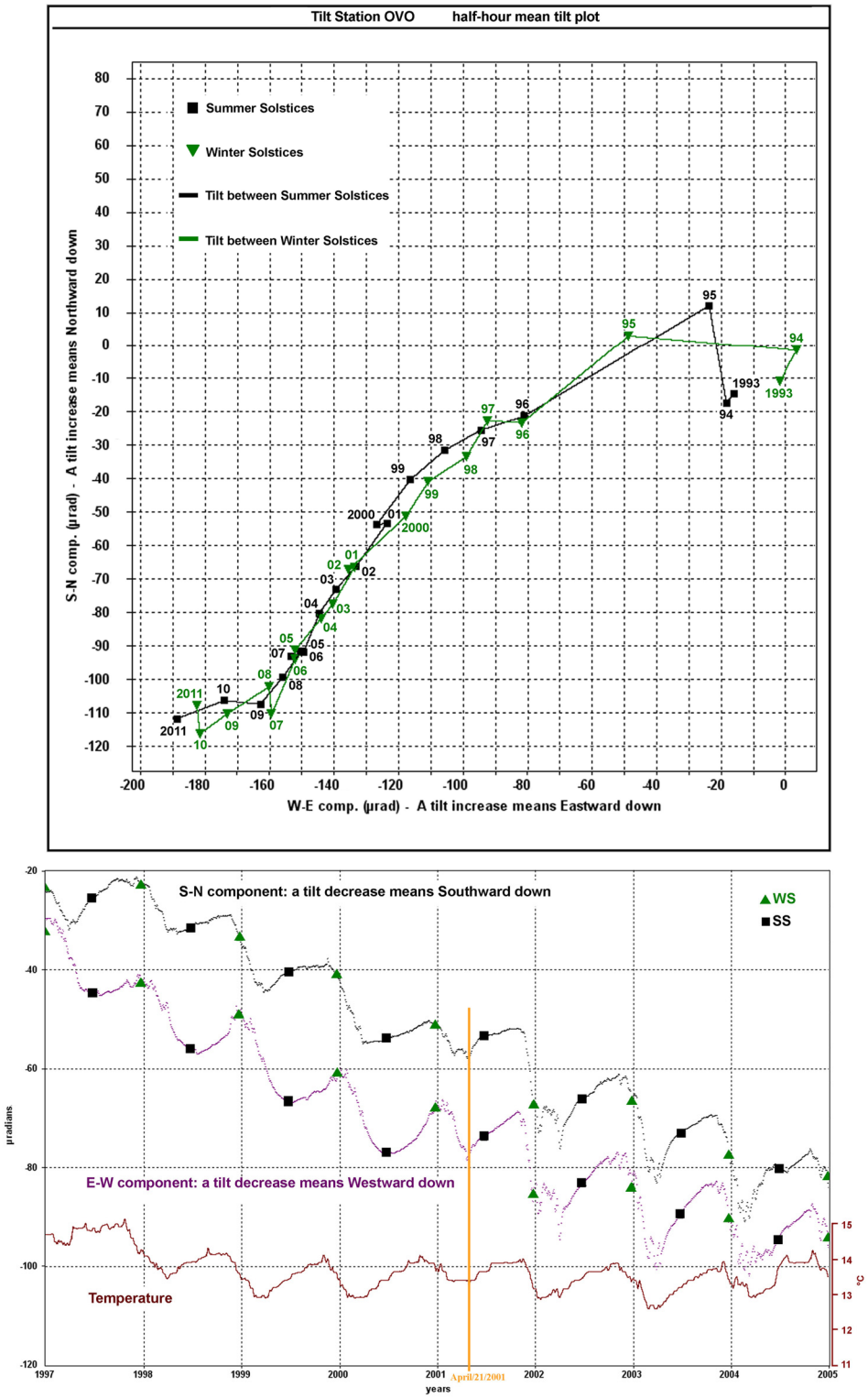

Figure 3. (a) Graph showing the tilt recorded at OVO station in the period from February 18, 1993, to May 27, 2012; on the same grid the Summer Solstices (SS) and the Winter Solstices (WS) are shown in order to point out how the ground thermo-elastic deformation induces some cyclicities and/or particular trends in the tiltmetric signal. Green and black segments define for each year the amplitude and directions of the tilt vector recorded respectively between WS and SS. (b) Tilt and thermal signals acquired at OVO for 1997-2005 to highlight the relationship between solar radiance and tilt response; on the same plot the Summer Solstices (SS) and the Winter Solstices (WS) are shown. We see a phase shift between the tilt signals and temperature, more evident in the W-E component, until April 21, 2001 (marked in orange) and then its total disappearance.

point recorded by the plot is defined by a pair of values ($Tilt^t_{EW}$, $Tilt^t_{NS}$) referred to time t. Each variation ($Tiltt^{+n}$ - $Tilt^t$) represents the ground tilt recorded over the nth time period characterized by both the amplitude and the direction. The adjustment and the orientation of the bi-axial sensors is accomplished in such a way that positive values indicate NE sinking and *vice versa*.

Tilt direction is calculated clockwise moving from

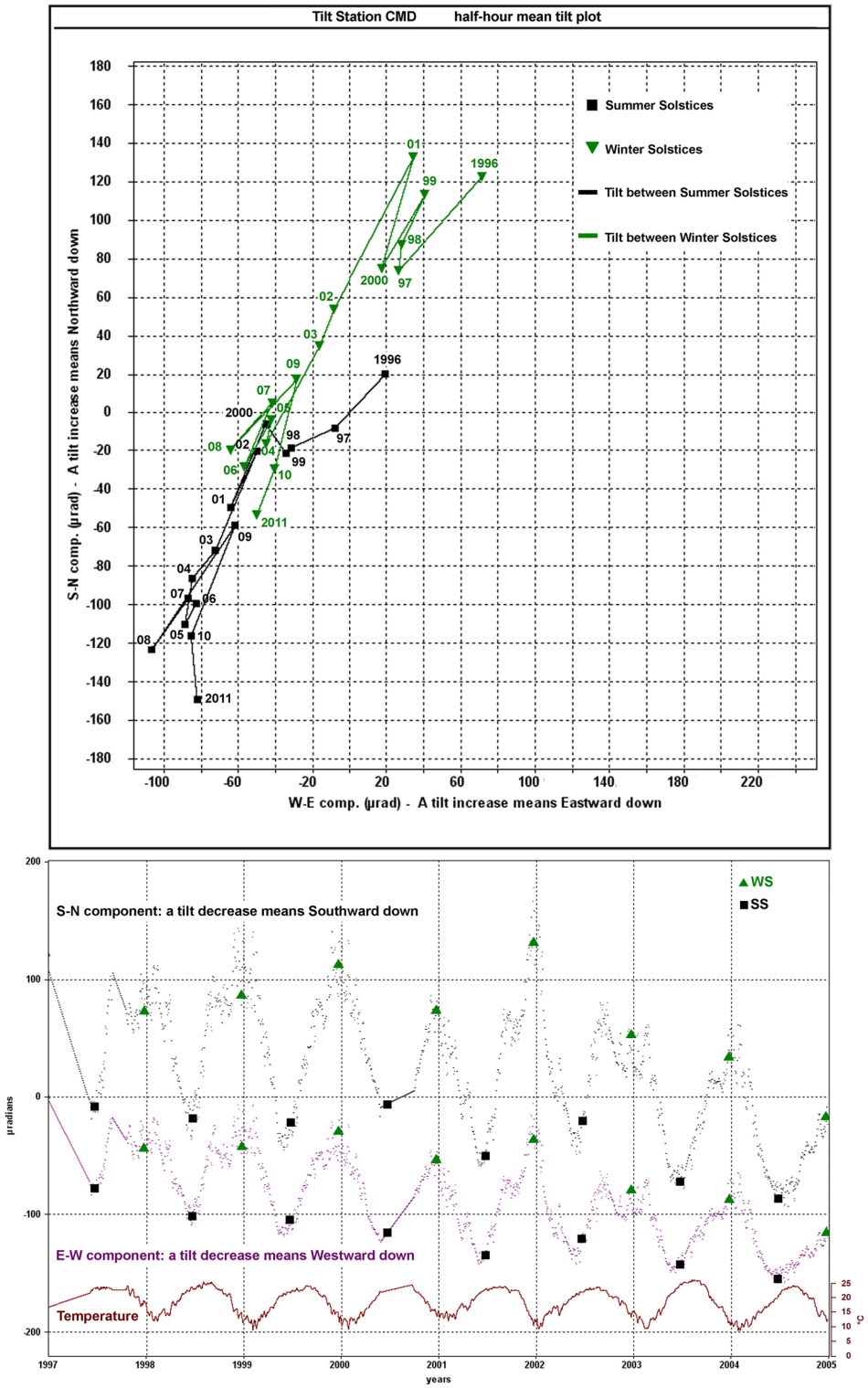

Figure 4. (a) Graph showing the tilt recorded at CMD station in the period from June 1st, 1996, to May 27, 2012; for further explanations see Figure 3a. (b) Tilt and thermal a signals acquired at CMD for 1997-2005: it is not evident a strong variation of phase shift between them.

N over time, whereas the percentage of counts of each recorded azimuth is shown by a frequency histogram.

Data processing uses graphic-analytical procedures and is organized following consecutive steps [Ricco et al. 2003, 2009]:

a) queuing of files downloaded from the server to data acquired from the start of the year;

b) reading of the updated data, wrong time acquisitions removal, linear interpolation of the missing data;

c) cleaning of the abrupt discontinuities on the signals (spikes), thermal compensation computed through the two coefficients K_s and K_z, conversion from mV to radians [AGI 1995];

d) two-dimensional representation of the tilt vector recorded by the station over time; graphs of the single components S-N, W-E, Te, atmospheric pressure, tilt

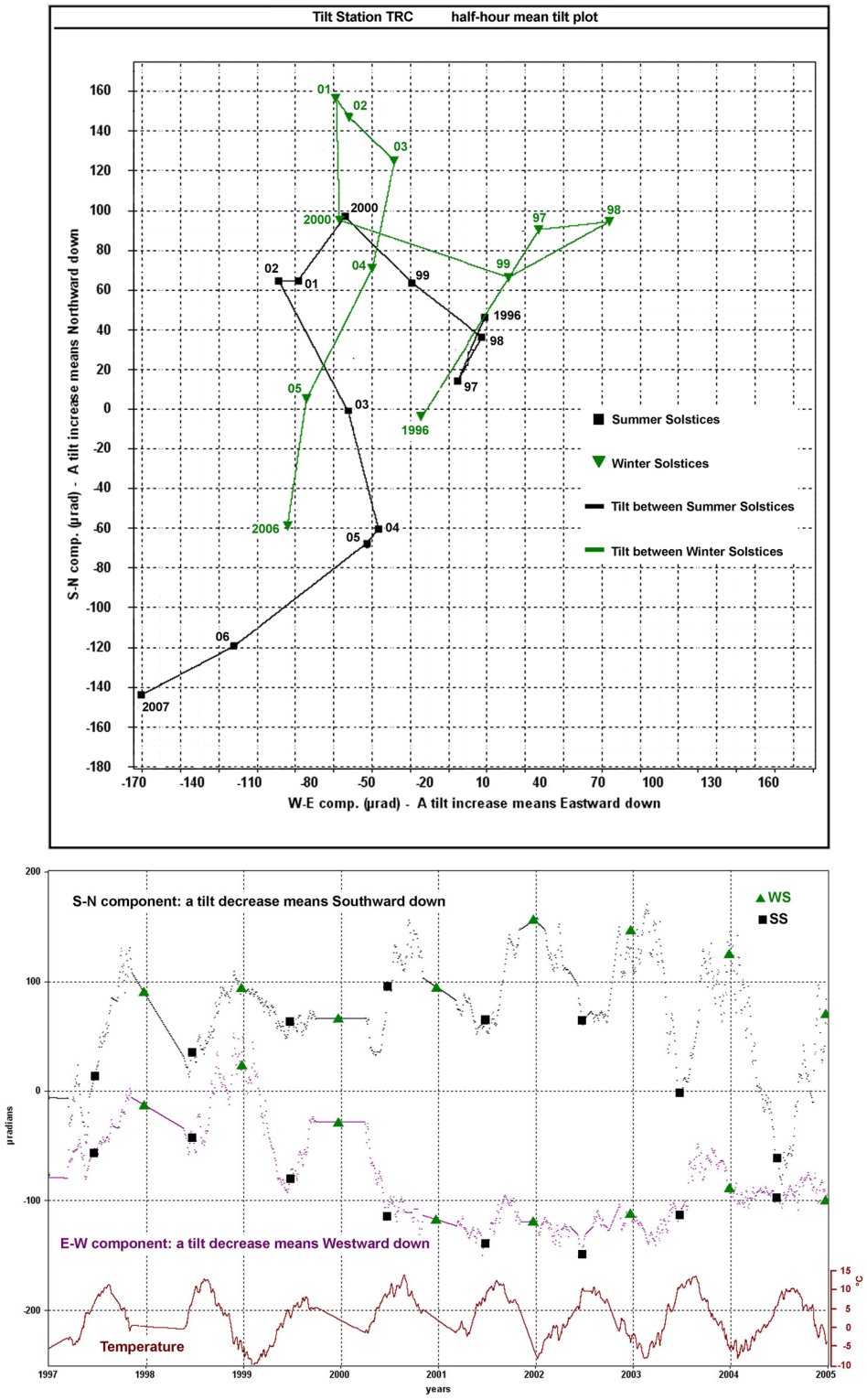

Figure 5. (a) Graph showing the tilt recorded at TRC station in the period from March 7, 1996, to June 11, 2007; for further explanations see Figure 3a. (b) Tilt and thermal signals acquired at TRC for 1997-2005 in which it is very clear the phase difference between tilt signals and temperature before and after April 21, 2001.

azimuth clockwise from N and relative frequency histogram of the azimuth;

e) power spectral density of acquired signals;

f) recorded tilt and atmospheric pressure signals with overlapping temperature in the same scale for the rough estimate of the degree of correlation between temperature and tilt or pressure and tilt.

6. Ground tilt pattern of the flanks of Mt. Vesuvius during the last 19 years

In this chapter the vector plots (hodograms) made with the tiltmetric signals recorded by the three vesuvius stations (step d) will be interpreted and discussed. In the grid representing the tilt field, every tic-interval corresponds to 20 μradians, furthermore the tilt in-

crease on S-N component must be interpreted as Northward down with respect to site station while the tilt increase on W-E component as Easthward down always with respect to it. For instance, a tilt increase in the S-N component at OVO and a decrease in the same component at CMD e TRC in conjunction with the tilt decrease in the W-E component at OVO and CMD and an increase in the same component at TRC could be a result of a crater inflation.

The OVO station shows that the tilting record occurs predominantly in the NE-SW direction (Figure 3a) and this is the typical direction also for the other two stations (CMD, Figure 4a, and TRC, Figure 5a). As a matter of fact, while the OVO station tilts almost always to SW and SSW, CMD and TRC stations tend to tilt alternatively to NE and SW; for the whole working period of the tilt stations, namely 19.28, 16 and 11.18 years, the three different sites show comparable tilt rates, that is 10.9, 13.5 and 11.3 μradians/year.

At this point we tried to qualitatively assess the influence of the annual temperature excursion, in the order of 1÷2 °C at OVO and of 18÷20 °C at CMD and TRC, on the thermo-elastic deformation of the rocks on which the tiltmeters are fixed, by dividing their operation period in the time intervals elapsed between the Summer Solstice (SS) and the Winter Solstice (WS) of each year and between the WS and SS of the following year. As it is known, since on the Summer Solstice the Sun reaches its maximum altitude, which is 72° 39′ degrees at a north latitude of 40° 48′ (Mt. Vesuvius), while on the Winter Solstice it is 25°45′, in the WS-SS period the day length increases and consequently the insolation hours whereas the opposite occurs in the SS-WS period.

In the hodograms shown in Figures 3a, 4a and 5a, on the grid of the tilts the SS and WS are also indicated in order to highlight possible cyclicities and/or trends induced into the tilt signal by solar radiation.

To highlight the relationship between solar radiance and tilt response, a period of 8 years (1997-2005) common to the 3 tilt stations was extracted, plotting for each of these tilt and thermal signals acquired and overlapping the Winter and Summer Solstices (Figures 3b, 4b and 5b).

In addition, to improve the understanding of hodograms the tilting directions for each station were computed, during the SS-WS and WS-SS time intervals (Table 1).

At OVO station the relationship between the two phenomena (insolation time and persistency in the same tilt direction) is weak in the SS-WS time intervals of each year as in 26% of these the ground tilts in the NE direction and in 42% of these in the SW direction, in the WS-SS time intervals conversely tilting occurs in SSW and SW directions in 61% of these (Table 1, Figure 3a,b).

The overall tilt recorded in the period from February

	Tilting direction (°) calculated clockwise moving from N	SS-WS time intervals	Tilting direction (°) calculated clockwise moving from N	WS-SS time intervals
TILT STATION OVO	75.2	1993	248.5	1993-1994
	54.3	1994	296.3	1994-1995
	249.8	1995	233.3	1995-1996
	197.1	1996	260.3	1996-1997
	37.2	1997	236.4	1997-1998
	104.1	1998	248.1	1998-1999
	95.2	1999	231.4	1999-2000
	74.2	2000	250.0	2000-2001
	220.3	2001	66.4	2001-2002
	247.2	2002	220.6	2002-2003
	190.6	2003	236.7	2003-2004
	162.4	2004	208.4	2004-2005
	278.8	2005	208.3	2005-2006
	123.2	2006	37.9	2006-2007
	205.9	2007	17.8	2007-2008
	235.6	2008	207.4	2008-2009
	254.3	2009	348.7	2009-2010
	217.6	2010	303.3	2010-2011
	57.2	2011		
TILT STATION CMD	26.8	1996	211.2	1996-1997
	22.9	1997	212.4	1997-1998
	29.5	1998	209.9	1998-1999
	29.2	1999	215.9	1999-2000
	37.7	2000	213.3	2000-2001
	28.5	2001	209.0	2001-2002
	29.2	2002	206.9	2002-2003
	27.7	2003	209.5	2003-2004
	29.6	2004	205.0	2004-2005
	23.6	2005	202.9	2005-2006
	20.1	2006	204.0	2006-2007
	23.9	2007	206.7	2007-2008
	22.2	2008	176.3	2008-2009
	23.6	2009	203.1	2009-2010
	27.4	2010	199.3	2010-2011
	18.6	2011		
TILT STATION TRC	213.5	1996	45.5	1996-1997
	29.4	1997	208.8	1997-1998
	48.8	1998	253.4	1998-1999
	86.9	1999	289.6	1999-2000
	239.7	2000	215.4	2000-2001
	12.3	2001	198.1	2001-2002
	23.9	2002	180.2	2002-2003
	10.9	2003	182.6	2003-2004
	358.7	2004	181.3	2004-2005
	336.8	2005	196.9	2005-2006
	24.8	2006	222.0	2006-2007

Table 1. Tilting directions observed during the SS-WS and WS-SS time intervals.

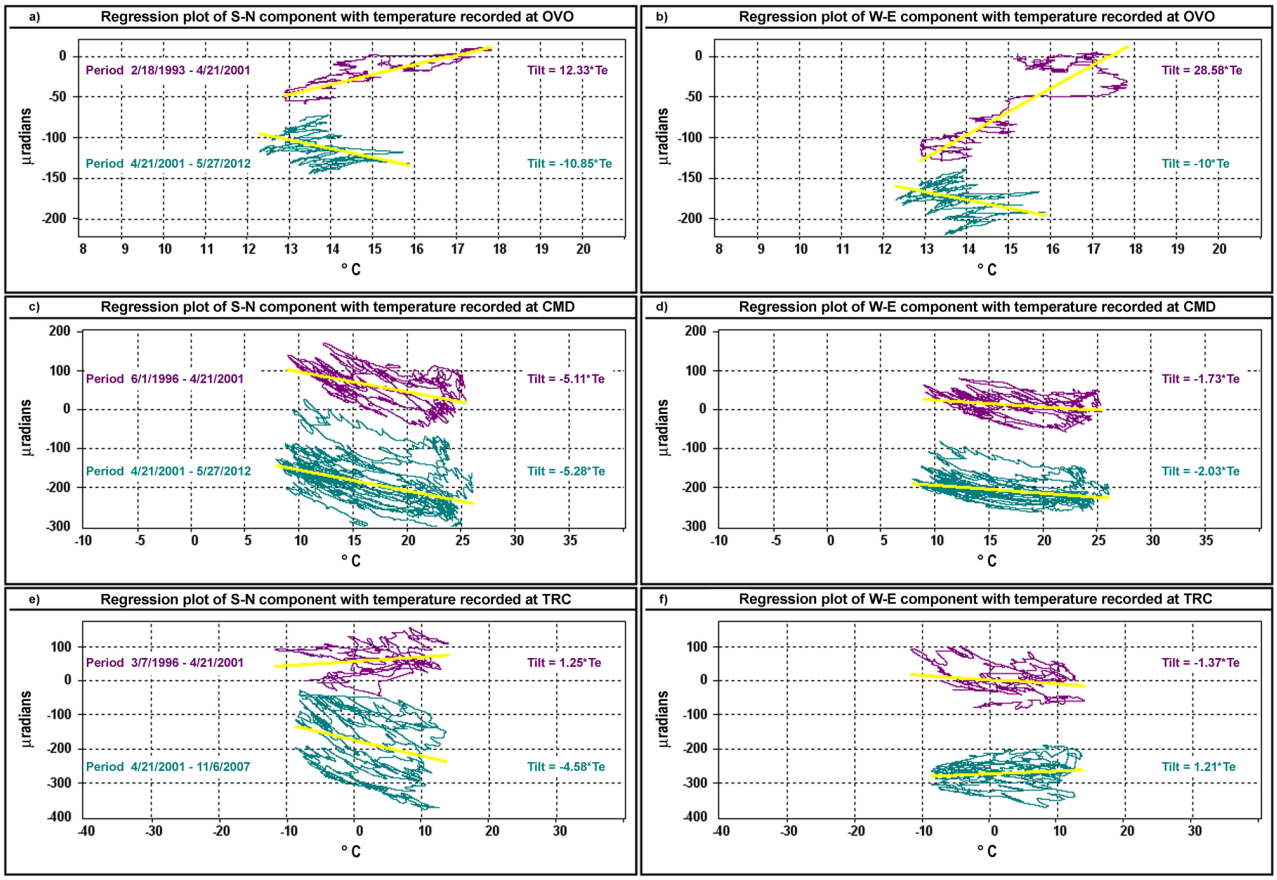

Figure 6. Regression plots of tilt components with temperature computed on two sets of data before ed after April 21, 2001, which indicate the sign change of the regression coefficient at OVO (Figure 6a,b) and at TRC (Figure 6e,f), while at CMD this sign remains unchanged (Figure 6c,d).

18, 1993, to May 27, 2012 is 210.5 µradians WSWward.

At CMD station clearly appears the dominance of tilting in the NNE direction in the SS-WS time intervals, namely when the insolation tends to decrease; in fact this phenomenon occurs in 100% of these whereas tilting occurs in SSW direction in 93% of the WS-SS time intervals (Table 1, Figure 4 a,b). This station has recorded in the period from June 1st, 1996, to May 27, 2012, an overall tilt of 216 µradians SSWward.

Also at TRC station the phenomenological relationship in the SS-WS time interval is weak as only in 45% of these the ground tilts in NNE direction, whereas such a relationship becomes more consistent in the WS-SS time intervals as tilting occurs in S, SSW directions in 73% of these; moreover this site is marked by a strong tilt dispersion in NW-SE direction (Table 1, Figure 5a,b). This station has recorded in the period from March 7, 1996, to November 6, 2007, an overall tilt of 130.6 µradians SWward.

Furthermore, by carefully analyzing the tilt and thermal signals acquired during the sub-period 1997-2005, we observe that the phase shift of the tilt signals with respects to the temperature begins to change gradually from the end of 2000, reaching a peak on April 21, 2001. This peculiarity is clear in Figure 3b where we see a phase shift between the signals until that date (marked in yellow) and then its total disappearance. This phenomenon is also found on the signals recorded by TRC (Figure 5b) and to a lesser extent on those recorded by CMD (Figure 4b).

To further characterize this phenomenon the equations for the lines of best fit from two sets of bivariate data (tilt/temperature recorded) were computed before and after this day, which indicate the sign change of the regression coefficient at OVO (Figure 6a,b) and TRC (Figure 6e,f), while at CMD this sign remains unchanged (Figure 6c,d).

The observation of the tilt pattern here discussed allows to summarize that, when the duration of the day increases during the first semester of each year resulting in a stronger solar radiation, the CMD tiltmetric station, located farthermost from Mt. Vesuvius crater, at a lower altitude closer to the coast line, tilts SSWward; the same behaviour, although less marked with the altitude increase, is observed at TRC and OVO stations.

Conversely, during the second semester, CMD station always rotates to NNE whereas, at higher altitudes, this direction always becomes less dominant; moreover the OVO station, topographically higher and with lower yearly thermal excursion tilts much more to SW than to NE.

Seasonal components and firstly thermal periodicities therefore strongly affect ground deformation

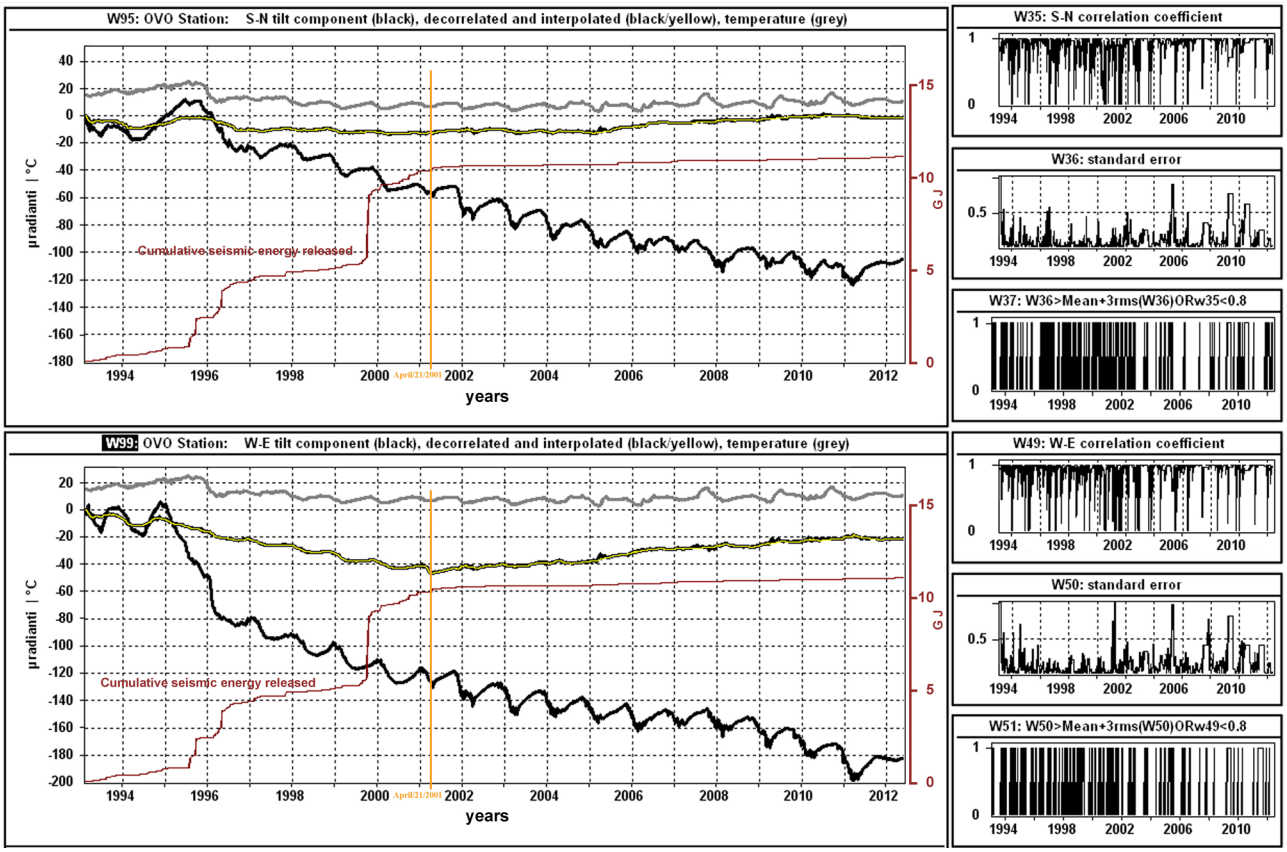

Figure 7. Application of a statistical procedure of thermal decorrelation to the S-N and W-E components of the tilt recorded by the OVO station through a polynomial dependence model. In the two windows on the left the signal recorded (black), the decorrelated (black) and interpolated (yellow) tilt sequence and temperature recorded (grey) are respectively shown for each component. The temperature plotted was rescaled multiplying by 4 and subtracting by 46 for enlarge it; moreover, to signals was superimposed in red the cumulative energy in 10^9 J released by earthquakes (Ml ≥2, Gutenberg and Richter relation; D'Auria et al. [2013]). The smaller windows on the right (window 37 and 51) report instead, in sequence for each component, the correlation coefficient *R* and the standard error of the estimate *es* between the regression polynomials and the filtered signals and also the operator $R < 0.8$ OR $es > 3\sigma$.

recorded by tiltmeters; such a restriction, however, represents also a strong point of tiltmetric monitoring as the scientist dealing with data interpretation will try to get information on the changes of the volcano dynamics from possible anomalies pointed out on a tilt signal correlated with the temperature. In fact the first research criterion carried out in the tilt analysis is to check the presence of repetitive deformation patterns on yearly basis and to study their interruptions and/or changes which could be related to other phenomena, usually endogenous.

7. Decorrelation procedure of the tilt signals

A second more quantitative criterion is used instead in the estimate and consequent removal of the systematic component of the ground tilt related to the thermo-elastic field, which is generated by temperature changes but is generally not in phase with this.

Because the temperature changes deform the ground in an unpredictable way due to its heterogeneity and therefore the thermo-elastic deformation of the ground surface layer on which the titmeters are placed is unknown, this influence can be evaluated and then subtracted only with a statistic approach that we called decorrelation which is a method able to quantify the ground tilt dependence on the temperature through a linear or a polynomial dependence model [Ricco et al. 2003, 2009].

This procedure is summarized below with the following steps:

a) Calculating the mean value of a set of 6 samples of the tilt and temperature signals (reducing the sample rate from 12 to 2 samples per hour) and convolution of the sequences thus obtained with a boxcar with a length of 4 days (equivalent to a moving average) after the addition of a certain number of null values at the ends of the same to avoid distortion effects.

b) Finding maximum and minimum values in the filtered thermal sequence in order to identify sub-sequences in either ascending or descending order, obtaining a set of values 0 1 where 1 (flags) identify the limits of the same portions of the signal. This calculation is not performed when the signal is missed for a period of more than 1 day, also the distance between the flags is set greater than 1 day to avoid fictitious extreme values.

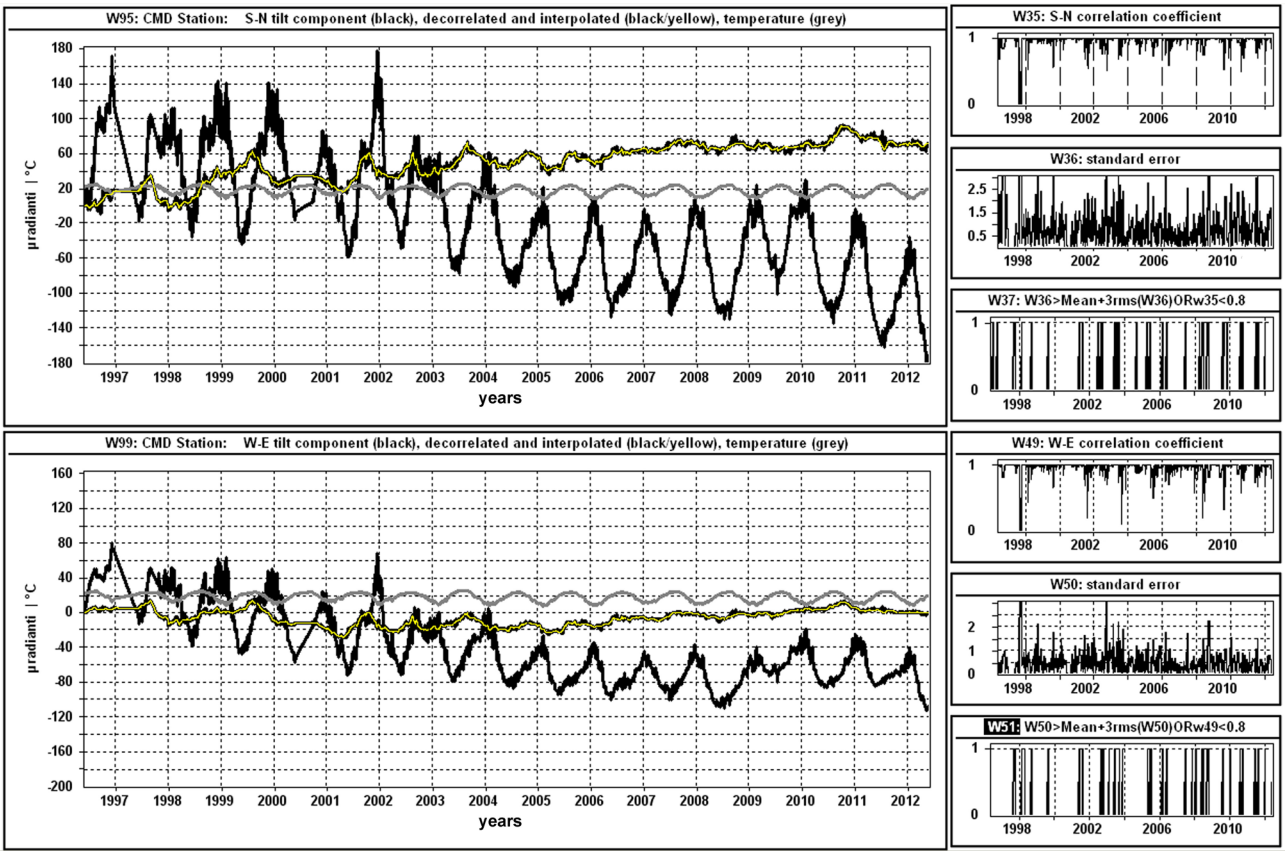

Figure 8. Application of a statistical procedure of thermal decorrelation to the S-N and W-E components of the tilt recorded by the CMD station (temperature not rescaled, for further explanations see Figure 7).

c) Decomposition of the filtered signals in *p* sub-sequences whose limits are identified by the flags taken from the set of values 0 1.

d) Polynomial regression of order 3 and 2 between the pairs of values (Te, SN) and (Te, WE) belonging to each sub-sequence, computation of the standard error of the estimate *es* and choice of the polynomial with lower *es*.

e) Computation of the residual values of the filtered signals with respect to the corresponding regression polynomials and reassembling of the whole sequence after eliminating the offset between adjacent sub-sequences.

f) Computation of a broken line joining the first and last values of the residual sub-sequences which in this model are the correct trend of the ground tilt.

g) Computation of the correlation coefficient R and *es* between the regression polynomials and filtered signals.

However, when tilt and temperature show very different waveforms or the signals are not in phase each other, *R* decreases and *es* increases; in this case these statistical indicators suggest that the polynomial fit is not acceptable.

For this reason it is considered unreliable the decorrelation of a given sequence in which $R < 0.8$ OR *es* falls outside the normal distribution built on the all *es* values (3σ).

The statistical decorrelation procedure of the tiltmetric sequences filtered with respect to the corresponding regression polynomials with the trend of the correlation coefficient, the standard error of the estimate and the OR logical operator between these two statistical indicators, is shown for the OVO station in Figure 7, for the CMD station in Figure 8 and for the TRC station in Figure 9.

At OVO station, decorrelation is not acceptable in 20.4% of the S-N sub-sequences and in 18.1% of the W-E ones (Figure 7, windows 37 and 51); it happens because in these signal intervals a phase displacement between tilt and temperature occurs, therefore a polynomial regression of order > 3 between the pairs of values Te, SN and Te, WE would be more adequate, but this procedure is not allowed by the decorrelation model that allows only the orders two or three.

At CMD station, decorrelation is not acceptable in 9.7% of the S-N sub-sequences and in 7.7% of the W-E ones (Figure 8, windows 37 and 51) while at TRC station the percentages are 8.5% for the S-N sub-sequences and 8% for the W-E ones (Figure 9, windows 37 and 51).

The phase displacement between the signals is therefore greater at OVO station and this can be appreciated from the trend of the *R* operator, showing lower values with respect to the other two stations (Figures 7, 8 and 9, windows 35 and 49); as instead the yearly ther-

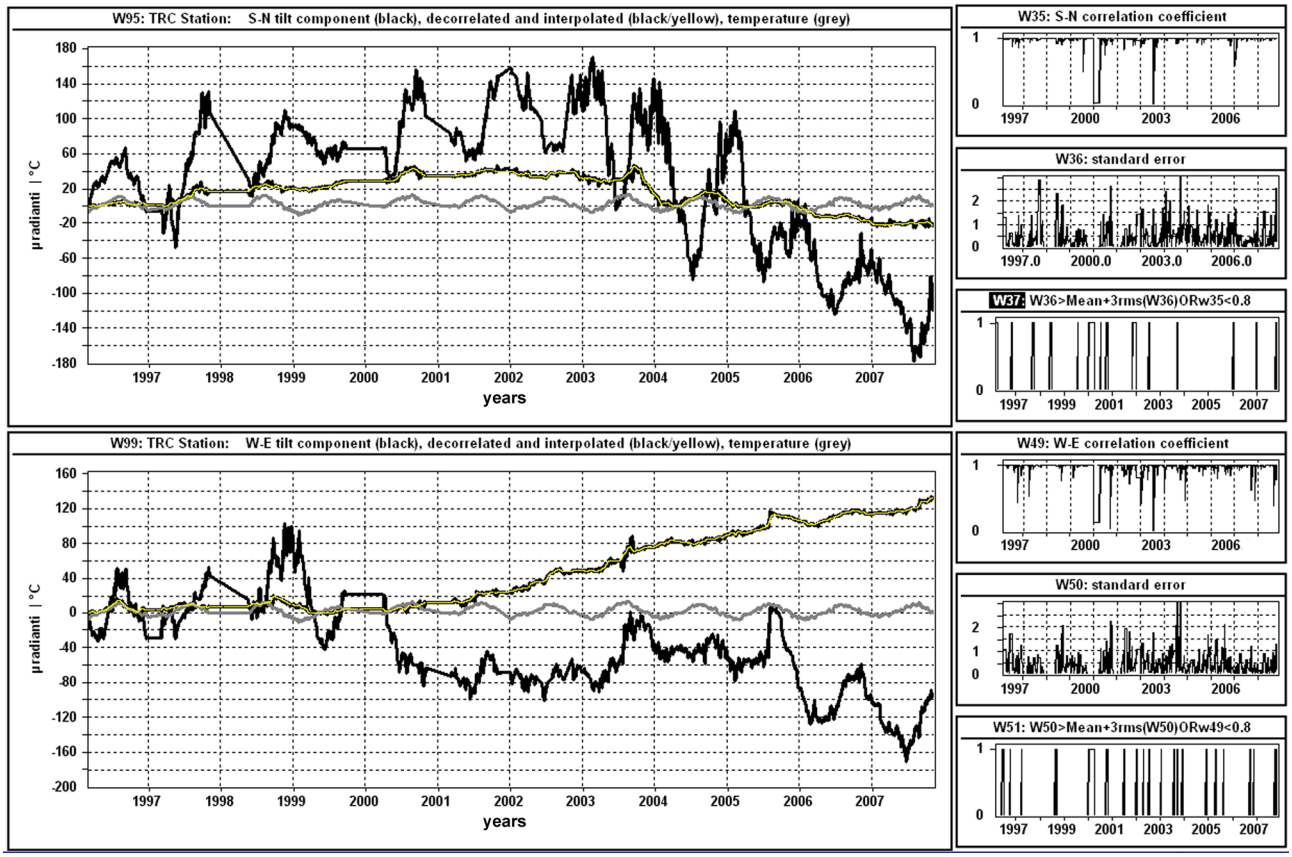

Figure 9. Application of a statistical procedure of thermal decorrelation to the S-N and W-E components of the tilt recorded by the TRC station (temperature not rescaled, for further explanations see Figure 7).

mal excursion at OVO station is about 1/10 of CMD and TRC stations, the residual values of the filtered signals with respect to the corresponding regression polynomials are usually lower and accordingly also the standard errors of the estimate *es* are lower (Figures 7, 8 and 9, windows 36 and 50).

Fortunately the S-N and W-E sub-sequences in which $R < 0.8$ *OR* $es > 3\sigma$ are short and temporally quite scattered along the whole tilt sequences; thereby no cumulative effects occur, that could result in wrong trends in the same sequences.

8. Interpretation of decorrelated data

The thermal decorrelation procedure applied to the tilt signals recorded by the three stations operating at Mt. Vesuvius has allowed to correct, within the limits of the method, the ground tilt recorded bringing it back to constant temperature conditions.

As regard to the OVO station, the correction procedure reduces the S-N tilt component by about 10 times and the W-E one by about 4 times; consequently the hodogram downsizes (Figure 10) compared to the one built from the recorded tilt signals (Figure 3a). As a matter of fact the tilt direction of this station, which is SW, SSWward in the original plot (Figure 3), becomes WSWward in the decorrelated one and remains the same till the end of 2000; starting from that time, tilt reverses the direction of 160° pointing NE till 2010 when it changes again the direction pointing SW as before (Figure 10). In the period 1993-2000, namely in 1995, a direction change occurs, clearly visible in the plot of Figure 10; among the three direction changes occurred in 1995, 2000 and 2010, the first and the last ones are clearly visible also in the plot of Figure 3a while the 2000 one is less clear.

The strong sign reversal of the trend seen at OVO between the end of 2000 and the first quarter of 2001 could be apparently surprising and likely due to artifacts in the correction procedure, but it is actually due to the change of the phase shift between the tilt and temperature signals (see Section 6); this anomaly is clearly visible in Figure 3b and causes the sign change of the regression coefficient shown in Figure 6a,b.

Since the temperature affects the recorded tilt, the decorrelation process (Section 7, steps b, c, d and e) that substantially operates comparing the phases of both signals produces, when changing the phase of one of the two, a sequence decorrelated with a trend different from that of the starting signal.

As a value of *R* greater than .8 was calculated for the sub-sequence relative to time interval April 19 to 25, while the error *es* is within the normal distribution, we believe this sign reversal is reliable.

It is therefore very important to identify the anomalies on the not decorrelated recorded signals; in fact

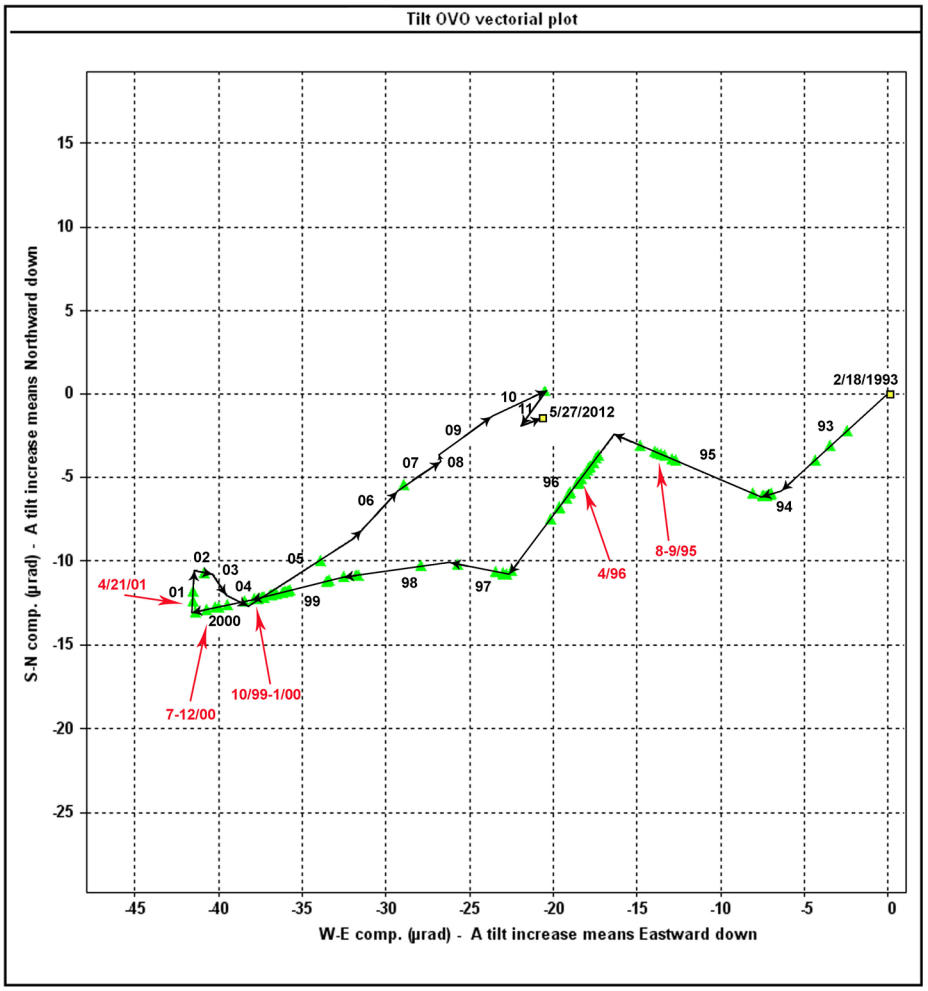

Figure 10. Graph of OVO station showing the hodogram of the decorrelated tilt in the period from February 2, 1993, to May 27, 2012; in this plot every tic-interval correspond to 5 μradians; black segments define for each year the amplitude of the tilt vector while the arrows give the direction in which the ground lowers. Moreover the overlapping light green triangles indicate the tilt computed during the periods, marked with red arrows, in which a daily seismic energy more than $14.4*10^9$ J has been released.

the repetitive deformation patterns on yearly basis, detectable on long series of tilt signals and primarily referred to thermal periodicities, can be modified by the occurrence of phenomena related to the volcano activity and therefore becoming anomalies in the not decorrelated signal.

At OVO station, such anomalies correspond to changes in the ground tilt direction that are detectable on both the original signals and the decorrelated tilt sequences; they coincide with two strong seismic crises that affected Mt. Vesuvius in the periods 1995-1996 and late 1999-2000, marked by average rate of energy release, respectively $0.9*10^{10}$J/month and $2.0*10^{10}$J/month on a background level observed before 1977 less than $0.1*10^{10}$J/month [De Natale et al. 2004].

The strong reversal of tilt direction seen at OVO between the end of 2000 and the first quarter of 2001 occurs at the beginning of a period of a consistent reduction of the energy released by vesuvius earthquakes. In order to show the contemporary nature of this phenomenon with the change in the ground tilt direction, in Figure 7 the cumulative energy in 10^9 J, released by earthquakes (Ml ≥2, Gutenberg and Richter relation; D'Auria et al. [2013]) recorded at Vesuvius from 1993, was superimposed.

The subsequent tilting of 2011 is not compatible with high seismic energy releases.

The correction procedure applied to CMD tilt station reduces the S-N and W-E components by approximately four times (Figure 11) and consequently the hodogram downsizes compared to the original one (Figure 4a).

The tilt direction is N, NW till the end of 2000; since then it gradually changes to NNE and this is the direction marking the original plot during the second semester of each year (Figure 4a); moreover after 2010 the tilt changes again as it rotates 180° and points SW (Figure 11). Everything suggests that this station, if it had been working in the time before 1996, it would have recorded also the 1995 anomaly during this seismic crisis; it is noteworthy, however, the direction change of about 60° (from NNW to NNE) during the strong in-

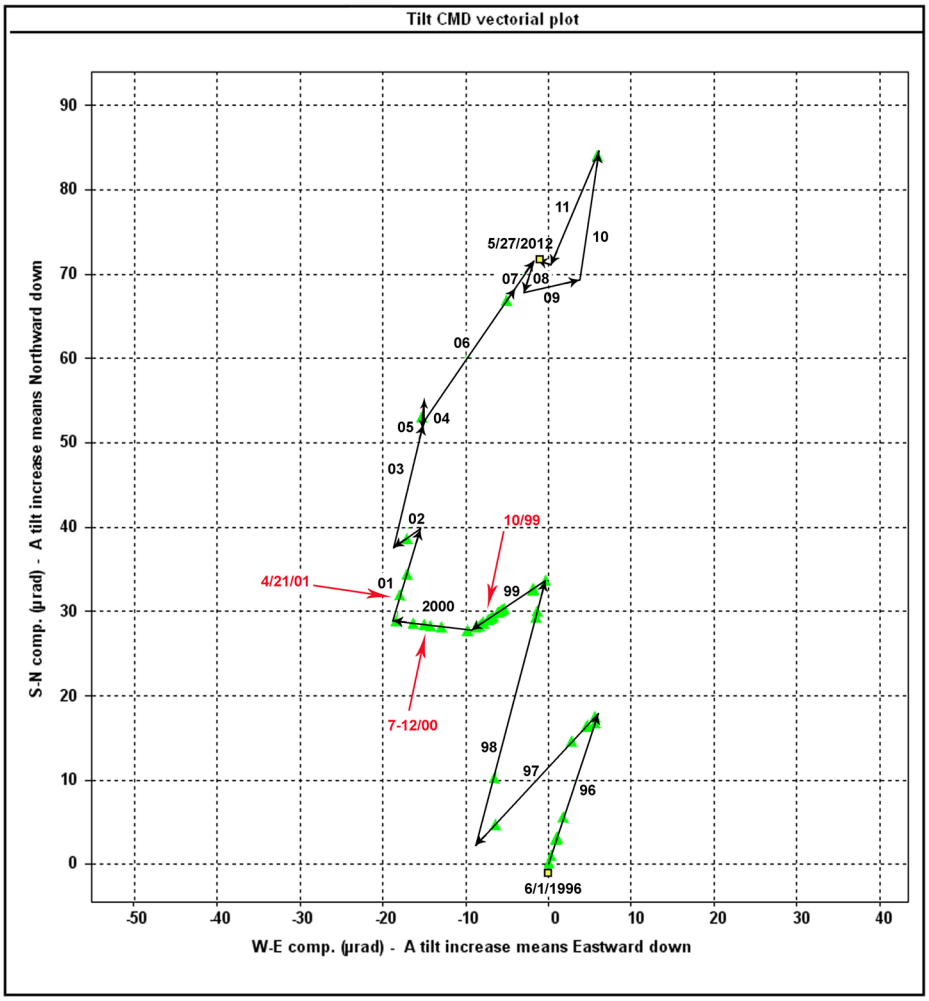

Figure 11. Graph of CMD station showing the hodogram of the decorrelated tilt in the period from June 1st, 1996, to May 27, 2012, in which every tic-interval corresponds to 10 μradians (for further explanations see Figure 10).

crease of seismicity occurred from the end of 1999 to the end of 2000.

As regard to TRC station, decorrelation reduces the S-N tilt component by approximately six times and the W-E one by approximately two times (Figure 12); also in this case the hodogram downsizes compared to the original one (Figure 5a).

The tilt direction remains N till the end of 2000; since then it gradually changes from NE to ESE and then to SE till 2007, when the station was removed; also at TRC station a direction change is observed, this time of about 100°, during the seismic crisis that affected Mt. Vesuvius in the period late 1999-2000 (Figure 12).

9. First results obtained from the data acquired by borehole tiltmeter

As mentioned before a Lily borehole tiltmeter was set up in Trecase close to the old TRC station abandoned in 2007 and this station was called with the same name of the one removed.

Signals recorded at TRC station by the new sensor were preliminarily analyzed to correct possible spikes or electrical transients and afterwards studied in the frequency domain to check its spectral content which must detect the solid earth tides on the tilt components and must not have periodicities of thermal type. The Lily sensor resolution, less than 5 nanoradians, allows in fact to record the tides that are on the order of 100 nanoradians [Melchior 1978]; moreover, at the depth in which the sensor is located, it is expected that thermal variations that usually produce elastic deformation in the ground are completely filtered, preventing to introduce solar periodicities or other cyclicalities in the recorded signals. In fact the only periodicities found in the tilt signals were the ones related to the K_1 diurnal luni-solar declinational (23.93 h) component, to the M_2 semi-diurnal principal lunar (12.42 h) component and to the K_2 semi-diurnal luni-solar declinational (11.97 h) component theoretically expected whereas on the thermal signal there was no evidence of the S_1 diurnal principal solar and S_2 semi-diurnal principal solar components (Figure 13).

From the analysis of the TRC station hodogram (Figure 14), we note an ESEward drift till December 28, 2011, afterwards a change in the tilt direction NWward

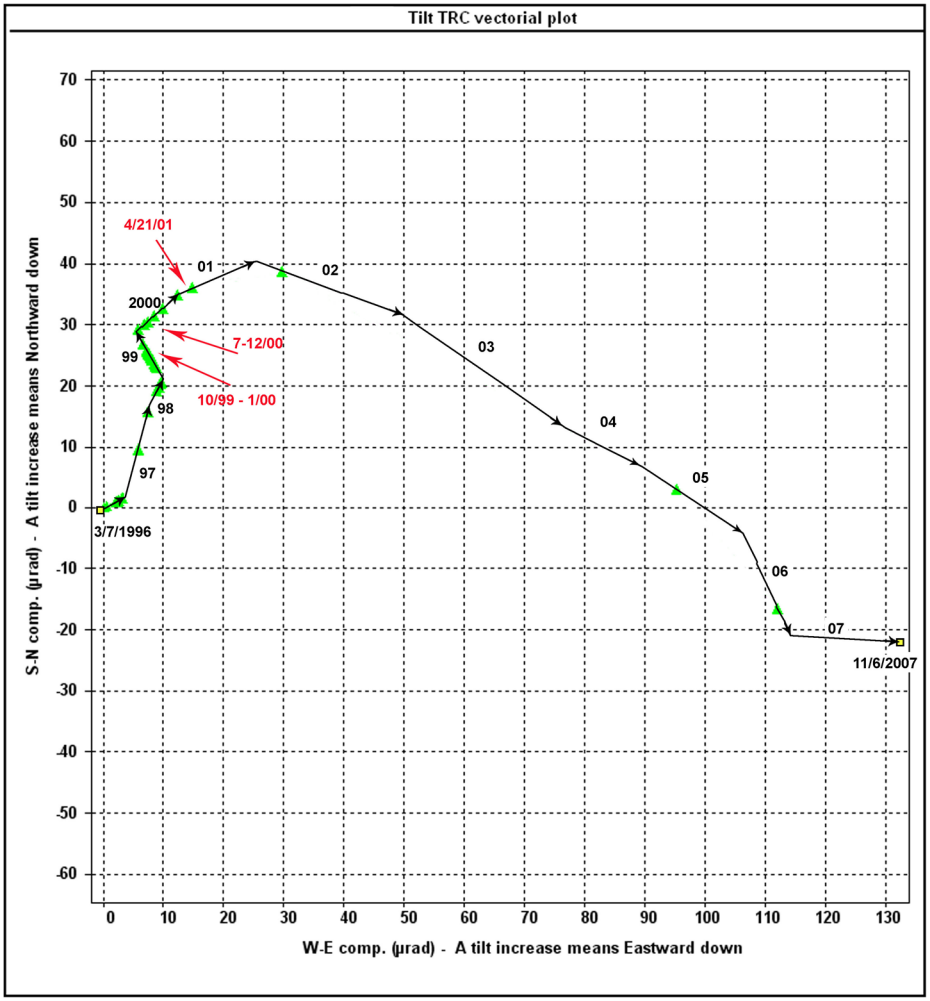

Figure 12. Graph of TRC station showing the hodogram of the decorrelated tilt in the period from March 7, 1996, to June 11, 2007, in which every tic-interval corresponds to 10 μradians (for further explanations see Figure 10).

lasted one week and then a renewal in the E direction; on February 13, 2012, the tilt suddenly changes rotating approximately 110° in SSW direction and then to WSW till March 9. At 20:31 UTC of the same day the tilt rotates again clockwise moving before to a NNE direction till the end of March, then to NE and lastly to E between April and May; on March 10 at 08:16 UTC a shallow 2.6 magnitude seismic event in the crater area was recorded.

The only anomaly pointed out during the sudden change of the tilt direction on February 13 refers to the temperature recorded by the thermal sensor 26 m deep, which undergoes on February 12 a decrease of 0.04 °C in about two days. This corresponds to less than 1/3 of the half-yearly thermal excursion and cannot be ascribed to any shallow thermal variation at depth.

10. Discussion

From the information obtained from the tiltmetric monitoring of three sites at Mt. Vesuvius covering a time span of 19.28 years on the north-western flank (OVO station), 16 years on the southern flank (CMD station) and 11.18 years on the south-eastern one (TRC station), a complex deformation pattern can be deduced, strongly dependent on the position of the sites in which the sensors were set up with respect to the morphology of the volcanic edifice and its structural outlines.

If we consider the signals as they were recorded, although previously corrected for the influences of the temperature on the sensors, the recorded tilting of the ground occurs mainly in the SW direction with tilt rates of about 11 μradians/year on both the western (OVO, 10.9 μradians/year) and eastern flanks (TRC, 11.3 μradians/year) of Mt. Vesuvius and of about 13 μradians/year on the southern one (CMD, 13.5 μradians/year) (Figures 3a, 5a and 4a). This direction marks the periods of the year in which the day length increases and consequently the insolation hours increase as well, i.e. in the time intervals elapsed between the Winter Solstice and the Summer Solstice of the following year.

This phenomenon is recorded almost always (in 93% of the cases) only at CMD station, located farther from Mt. Vesuvius crater, at a lower altitude and consequently closer to the coast line whereas it becomes a little less marked but it is also present with increasing al-

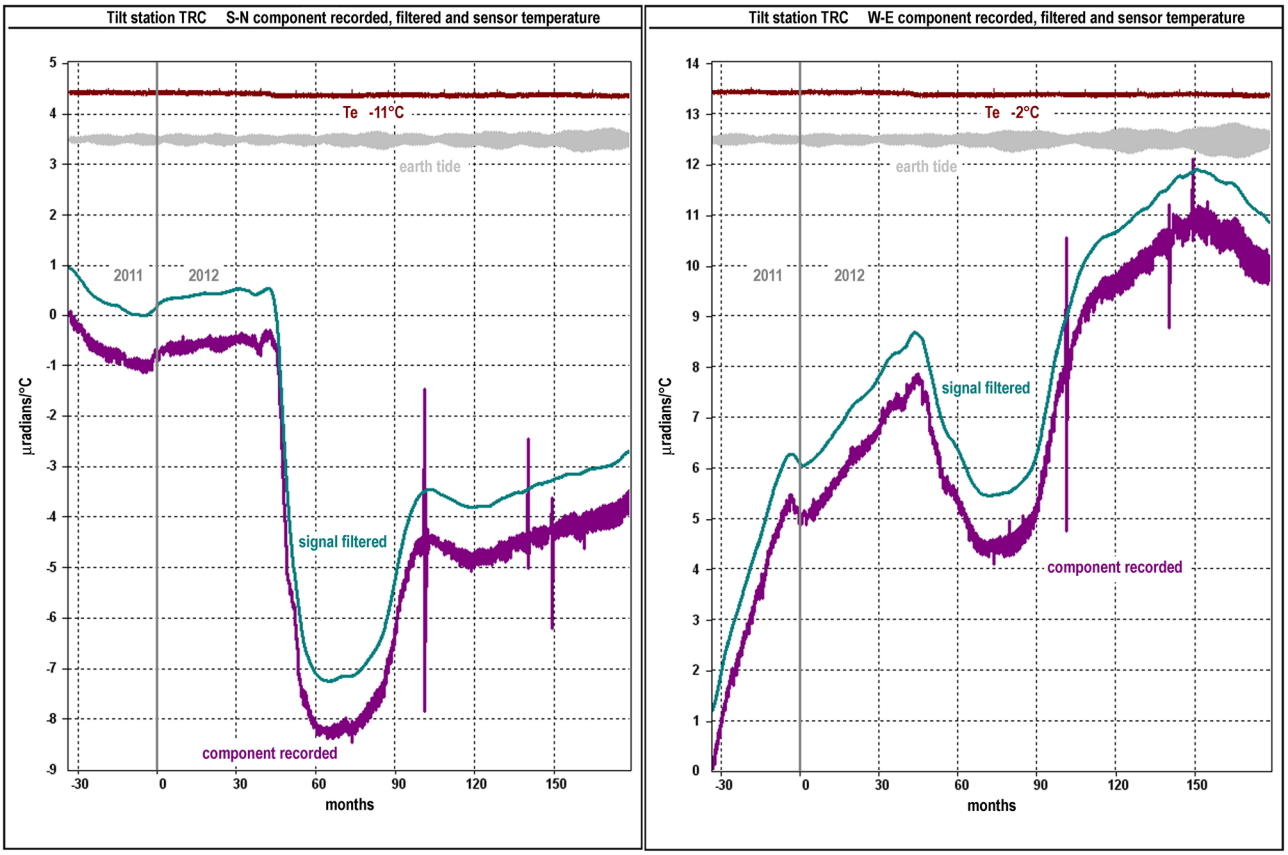

Figure 13. S-N (left) and W-E (right) components of TRC station. The recorded signals are in violet, the temperature in red, the trend components in green and in grey the earth tides in the tidal-frequencies twice-daily and daily (11.86÷12.48 and 23.45÷24.69 hours).

titude, as this is observed in 73% of the cases at TRC station and in 61% of the cases at OVO station. *Vice versa*, during the periods of the year in which the day length and insolation decrease (Summer-Winter Solstices), the prevailing tilt direction is the opposite NE which is recorded in 100% of the cases at CMD station whereas it becomes less dominant going high (45% a TRC station and 26% at OVO station).

The SW tilting recorded by tiltmeters occurs therefore irregularly and shows some seasonalities, consistent with the solar thermal radiation causing the thermoelastic effect measured by sensors, but that could be also due to displacements of underground masses, e.g. aquifers; in fact it is known from literature that the variation in acquifer level can induce signals in geodetic measurements [Kumpel 1983, Braitenberg 1999]. Regarding the Vesuvius volcanic area, however, records of water wells are not available at the time, that can prove this assumption.

The removal by statistical procedure of the seasonal effects (decorrelation) outlines on the contrary a different but equally interesting deformation field as it shows interruptions with changes in both trend and amplitude during two periods of strong seismic activity that affected Mt. Vesuvius in the periods 1995-1996 and late 1999-2000, marked by an average rate of energy release of at least one order of magnitude greater than the previous and following periods.

Till 2000, 43 radians in WSW direction were computed, with a tilt rate of 5.5 µradians/year at OVO station, 34.8 µradians in NW direction with a tilt rate of 7.6 µradians/year at CMD station and 39 µradians in NNE direction with a tilt rate of 8 µradians/year at TRC station. Starting from that year tilting changes in both modulus and direction, as 25.4 µradians in NE direction have been computed, with a tilt rate of 2.5 µradians/year at OVO station, 61.3 µradians in NNE direction with a tilt rate of 6.1 µradians/year at CMD station and 133 µradians in SE direction with a tilt rate of 20.5 µradians/year at TRC station (Figures 10, 11 and 12).

After 2000, a yearly deceleration of tilting (55%) occurs on the north-western flank (OVO station), a lower deceleration (20%) on the southern flank (CMD station) but a strong acceleration of tilting (about 2.5 times higher than the one before 2000) occurs on the south-eastern flank (TRC station) of the volcano.

Although TRC station was dismissed in November 2007, exactly four years later it was replaced with a borehole tiltmeter at 26 m depth whose data, with no thermal drift, allow to give the same tilting direction (SE) with a tilt rate of 18 µradians/year (Figure 14); these values are therefore strictly comparable with those cal-

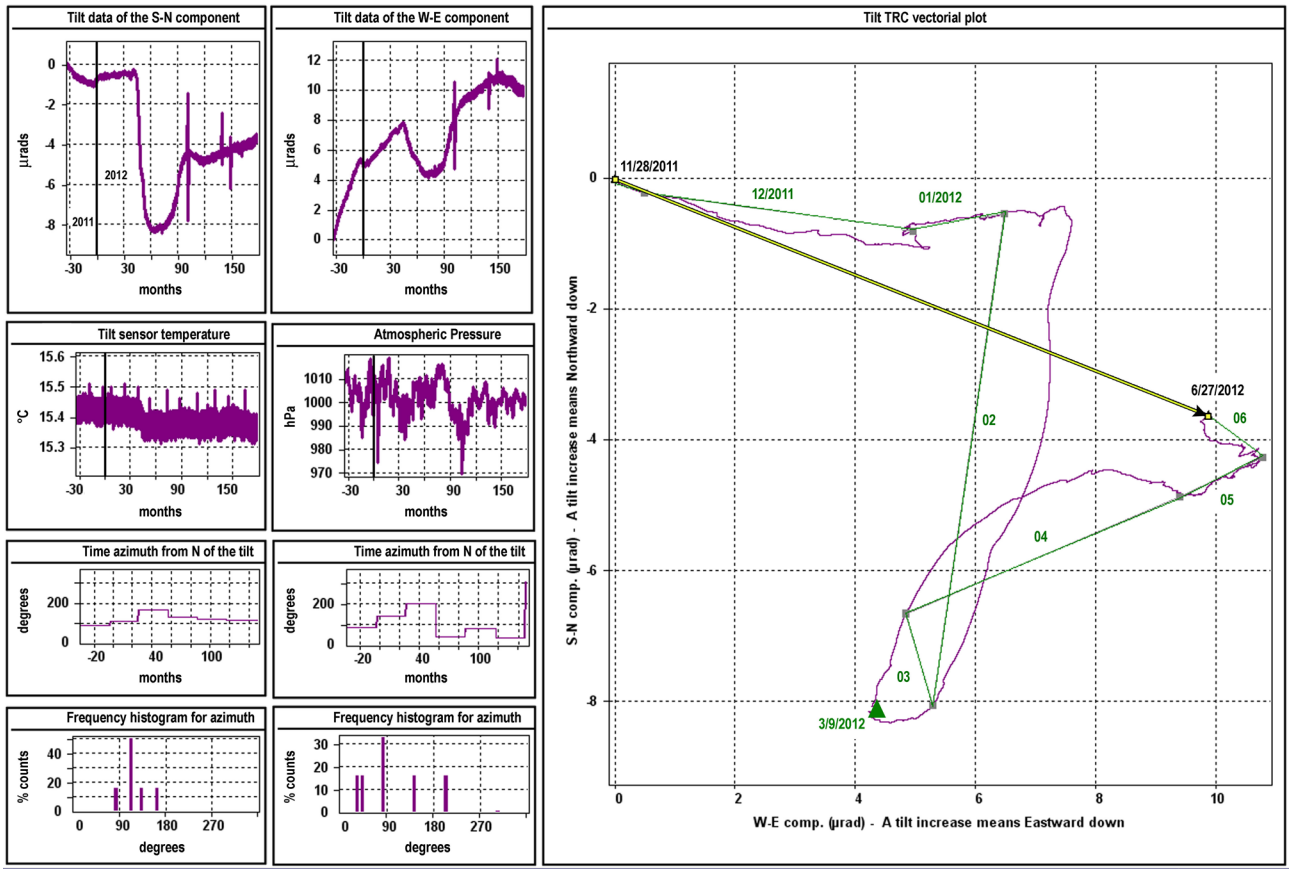

Figure 14. This worksheet shows the signals recorded by the new TRC station and other parameters derived from them. In the 8 windows on the left are reported respectively clockwise tilt data of the S-N component, tilt data of the W-E component, atmospheric pressure recorded at CMD station, time azimuth from N of the tilt in the range t(n)- t(n-1) and the relative frequency histogram, frequency histogram of the time azimuth from N of the tilt in the range t(n)-t(0) and relative azimuth, Lily temperature. On the right the hodogram with tic-intervals every 2 µradians is shown; green segments define for each month the tilt amplitude and direction while the overlapping black-yellow line give the tilt amplitude in the time interval November 28, 2011, to June 27, 2012, and the arrow give the direction in which the ground lowers. The green triangle indicates the period in which a daily seismic energy more than $14.4*10^9$ J has been released.

culated from 2001 to 2007 from the signals recorded by the old sensor (Figure 12).

The change in intensity and direction of the deformation detected by tiltmeters since 2001 is related with the variations of the phase shift between the tilt components and the temperature recorded, compared to previous years. This change, visible on the original hodograms (position of black squares 2000 and 2001 on the grid of Figures 3a, 4a and 5a) is stronger at OVO (Figure 3b) and TRC (Figure 5b) and less clear in CMD (Figure 4b), and takes place after the second week of April 2011. The consequent thermal correction applied to the recorded signals produce decorrelated sequences that show vectorially the sign reversal of the trend seen between the end of 2000 and the first quarter of 2001 (Figures 10, 11 and 12).

In this period we observed a strong decrease of the energy released by vesuvius earthquakes (Figure 7) and this observation suggests a link between the two phenomena. Such a phenomenological relationship is also observed in the data recorded at TRC station by the borehole tiltmeter where even the clockwise rotation of the tilting direction recorded on March 9, 2012, occurs about 12 hours before a shallow 2.6 magnitude seismic event in the crater area (Figure 14).

11. Conclusions

In this paper we analyzed tilt observations at Vesuvius from 1993 to the present. We have shown the network installation, its evolution over time and the gradual transition from surface sensors to boreholes. Although only one borehole has been installed to a depth of 26 m, three more wells drilled at depths ranging from 20 to 26 m around Mt. Vesuvius crater at altitudes between 760 and 970 m a.s.l. (Figure 2) will also allow to get high quality data, leading to further progress in the knowledge of the dynamics of this dangerous volcano.

We have processed the signals recorded by surface tiltmeters using a statistical procedure that allowed us to bring the ground tilt recorded to constant temperature conditions and analyzed both the original signals and the uncorrelated sequences. In this way, we collected three different types of information: the first one derived by ground tilting mainly conditioned by the

Figure 15. Tilt rate in µradians/year calculated at three sites before and after 2000; the vectors point towards the subsiding area.

thermo-elastic deformation and therefore directly connected to solar insolation, the second one resulting from the thermal correction and therefore to the true deformation of the volcano, and finally the last one inferred from the study of the clean signal recorded at 26 m depth. The latter, unfortunately, covers only a time span of about 7 months compared with the others (about 19, 16 and 11 years).

The first dataset (not corrected from temperature) shows a ground tilting mainly in the SW direction with tilt rates of about 11 µradians/year on both western and eastern flanks of Mt. Vesuvius and of about 13 µradians/year on the southern one (Figures 3a, 4a and 5a). Because tilt vectors point in the long term outward from the summit and towards the subsiding area, this supports the hypothesis of a southern areas subsidence.

This phenomenon has been observed also through other geodetical data as ERS InSAR data, GPS data and levelling surveys [Lanari et al. 2002], thus characterizing the southwestern part of the Somma-Vesuvius volcanic complex that is lower than 600 meters with respect to the northern one; this morphological lowering, deduced by from meso-structural and geophysical studies, may be due the NW-SE trending tectonic structure dipping SSWward [Cassano and La Torre 1987, Bianco et al. 1998] Afterwards, Borgia et al. [2005] interpret the subsidence as related to a spreading effect of Vesuvius, taking into account many geological and geophysical data.

The second dataset (corrected from temperature) shows before 2001 a tilt rate of 5.5 µradians/year in WSW direction on the western flank, 8 µradians/year in NNE direction on the eastern flank and 7.6 µradians/year in NW direction on the southern one (Figures 10, 11, 12 and 15).

These tilting directions must be interpreted considering the complexity of the deformation pattern outlined from the joint analysis of InSAR and optical levelling data, which show the subsidence effects of a semicircular narrow strip around the volcanic edifice and of the summit part of the crater and a regional scale subsidence, with the SE sector moving eastwards with respect to the NW one.

Also, tilting change in intensity and direction resulting from the second dataset and connected with the variations of the phase shift between the tilt components and the temperature recorded, compared to previous years, begins after the second week of April 2011 in conjunction with a strong decrease of the energy released by vesuvius earthquakes. From this data we estimate a tilt rate of 2.5 µradians/year in NE direction on the western flank, 20.5 µradians/year in SE direction on the eastern flank and 6.1 µradians/year in NNE direction on the southern one (Figures 10, 11, 12 and 15).

Finally, the last dataset contains signals recorded at depth on the eastern flank of the volcano which confirm the tilting direction (SE) and the rate of the same order of magnitude (18 µradians/year) (Figure 14).

The results we got so far from tiltmetric monitoring at Mt. Vesuvius therefore highlight a complex and interesting deformation field; moreover the seismic events/ tilt changes associations found till now allow us to mark an important link between the major

changes in the direction of the tilt vectors and seismic activity. This phenomenological relationship is observed in correspondence with strong gradients in both positive and negative energy release of earthquakes and therefore deserves an adequate seismological investigation.

References

AGI (1988). 700-Series platform and surface mount tiltmeters, User's Manual, no. B-88-1016, Rev. E.

AGI (1995). Tiltmeter temperature coefficients: source, definition and use to improve accuracy, Technical report no. B-95-1005, Rev. C.

AGI (2001). Model 798-A Handi-Logger User's Manual TelephoneTelemetry Option, User's Manual, no. B-01-1008, Rev. E.

AGI (2005). LILY Self-Leveling Borehole Tiltmeter User's Manual, no. B-05-1003, Rev. D.

Aprile, F., and F. Ortolani (1979). Sulla struttura profonda della Piana Campana/ Deep structure of the Campana Plain, Boll. Soc. Nat. Napoli, 88, 243-261.

Aquino, I., C. Ricco and C. Del Gaudio (2006). Rete tiltmetrica dell'area napoletana, Open File Report INGV, 4.

Arnò, V., C. Principe, M. Rosi, R. Santacroce, A. Sbrana and M.F. Sheridan (1987). Eruptive history, In: R. Santacroce (ed.), Somma-Vesuvius, Quaderni de "La Ricerca Scientifica", CNR, 114, 53-103.

Arrighi, S., C. Principe and M. Rosi (2001). Violent strombolian and subplinian eruptions at Vesuvius during post-1631 activity, Bull. Volcanol., 63, 126-150.

Berardino, P., G. Fornaro, R. Lanari and E. Sansosti (2002). A new algorithm for surface deformation monitoring based on small baseline differential SAR interferograms, IEEE Trans. Geosci. Remote Sens., 40, 2375-2383.

Bianco, F., M. Castellano, G. Milano, G. Ventura and G. Vilardo (1998). The Somma-Vesuvius stress field induced by regional tectonics: evidences from seismological and mesostructural data, J. Volcanol. Geoth. Res., 82, 199-218.

Borgia, A., P. Tizzani, G. Solaro, M. Manzo, F. Casu, G. Luongo, A. Pepe, P. Berardino, G. Fornaro, E. Sansosti, G.P. Ricciardi, N. Fusi, G. Di Donna and R. Lanari (2005). Volcanic spreading of Vesuvius, a new paradigm for interpreting its volcanic activity, Geophys. Res. Lett., 32, L03303; doi:10.1029/2004GL02 2155.

Braitenberg, C. (1999). Estimating the hydrologic induced signal in geodetic measurements with predicitive filtering methods, Geophys. Res. Lett., 26, 775-778.

Braitenberg, C., I. Nagy, M. Negusini, C. Romagnoli, M. Zadro and S. Zerbini (2001). Geodetic measurements at the northern border of the Adria plate, Millennium Issue of the Journal of Geodynamics, 32 (1/2), 267-286.

Cassano, E., and P. La Torre (1987). Geophysics, In: R. Santacroce (ed.), Somma-Vesuvius, Quaderni de "La Ricerca Scientifica", CNR, 114, 175-196.

Cioni, R., R. Santacroce and A. Sbrana (1999). Pyroclastic deposits as a guide for reconstruction the multi-stage evolution of the Somma Vesuvius Caldera, Bull. Volcanol., 61, 207-222.

D'Auria, L., A.M. Esposito, D. Lo Bascio, P. Ricciolino, F. Giudicepietro, M. Martini, T. Caputo, W. De Cesare, M. Orazi, R. Peluso, G. Scarpato, C. Buonocunto, M. Capello and A. Caputo (2013) The recent seismicity of Mt. Vesuvius: inference on seismogenic processes, Annals of Geophysics, 56 (4), S0453; doi:10.4401/ag-6448.

De Natale, G., I. Kuznetzov, T. Kronrod, A. Peresan, A. Saraò, C. Troise and G.F. Panza (2004). Three Decades of Seismic Activity at Mt. Vesuvius: 1972-2000, Pure Appl. Geophys., 161, 123-144.

Doglioni, C. (1991). A proposal for kinematic modeling of W-dipping subductions-possible applications to the Tyrrhenian-Apennines system, Terra Nova, 3, 426-434.

Dzurisin, D. (1992). Electronic tiltmeters for volcano monitoring: Lessons from Mount St. Helens, U.S.G.S. Bulletin, 69-83.

Ferro, A., S. Gambino, S. Panepinto, G. Falzone, G. Laudani and B. Ducarme (2011). High Precision Tilt Observation at Mt. Etna Volcano, Italy, Acta Geophysica, 59 (3), 618-632; doi:10.2478/s11600-011-0003-7.

Gambino, S., O. Campisi, G. Falzone, A. Ferro, F. Guglielmino, G. Laudani and B. Saraceno (2007). Tilt measurements at Vulcano Island, Annals of Geophysics, 50 (2), 233-247.

Genco, R., and M. Ripepe (2010). Inflation-deflation cycles revealed by tilt and seismic records at Stromboli volcano, Geophy. Res. Lett., 37, L12302; doi:10.1029/2010GL042925.

Grillo, B., C. Braitenberg, R. Devoti and I. Nagy (2011). The study of Karstic aquifers by geodetic mesurements in Bus de la Genziana station – Cansiglio Plateau (Northeastern Italy), Acta Carsologica, 40 (1), 161-173.

Harrison, J.C. (1976). Cavity and topographic effects in tilt and strain measurements, J. Geophys. Res., 81, 319-328.

Harrison, J.C., and K. Herbst (1977). Thermoelastic strains and tilts revised, Geophys. Res. Lett., 535-537.

Imbò, G. (1939). Oscillazioni dell'edificio vulcanico concomitanti le recrudescenze eruttive del vul-

cano, Rendiconti della R. Accademia Nazionale dei Lincei, XXIX.

Ippolito, F., F. Ortolani and M. Russo (1973). Struttura marginale tirrenica dell'Appennino Campano; reinterpretazione di dati di antiche ricerche di idrocarburi, Mem. Soc. Geol. Ital., 12, 27-250.

Jentzsch, G., M. Liebing and A. Weise (1993). Deep boreholes for high resolution tilt recordings, Bull. Inf. Marees Terr., 115, 8498-8506.

Kumpel, H.J. (1983). The Effect of Variations on the Groundwater Table on Borehole Tiltmeters, In: J.T. Kuo (ed.), Proc. 9th Int. Symp. Earth Tides (New York, 1981), 33-45.

Lanari, R., G. De Natale, P. Berardino, E. Sansosti, G.P. Ricciardi, S. Borgstrom, P. Capuano, F. Pingue and C. Troise (2002). Evidence for a peculiar style of ground deformation inferred at Vesuvius volcano, Geophys. Res. Lett., 29 (9), doi:10.1029/2001GL 014571.

Melchior, P. (1978). The Tides of the Planet Earth, Pergamon Press.

Pescatore, T.S., and I. Sgrosso (1973). I rapporti tra la piattaforma campano-lucana e la piattaforma abruzzese-campana nel casertano, Boll. Soc. Geol. It., 92, 925-938.

Ricco, C., I. Aquino and C. Del Gaudio (2003). Ground tilt monitoring at Phlegraean Fields (Italy): a methodological approach, Annals of Geophysics, 46 (6), 1297-1314.

Ricco, C., I. Aquino and C. Del Gaudio (2009). Procedura automatica per lo sudio dei segnali registrati da una stazione tiltmetrica, Rapporti Tecnici INGV, 115.

Rolandi, G., P. Petrosino, and J. Mc Geehin (1998), The interplinian activity at Somma-Vesuvius in the last 3500 years, J. Volcanol. Geoth. Res., 82, 19-52.

Rosi, M., C. Principe and R. Vecci (1993). The 1631 Vesuvius eruption – a reconstruction based on historical and stratigraphical data, J. Volcanol. Geoth. Res., 58, 151-182.

Santacroce, R., ed. (1987). Somma-Vesuvius, Quaderni de "La Ricerca Scientifica", CNR, 114 (Progetto finalizzato Geodinamica, Monografie finali, 8), 251 pp.

Scandone, P. (1979). Origin of the Tyrrhenian sea and Calabrian arc, Boll. Soc. Geol. It., 98, 27-34.

Tenze, D., C. Braitenberg and I. Nagy (2012). Karst deformations due to environmental factors: evidences from the horizontal pendulums of Grotta Gigante, Italy. Bollettino di Geofisica Teorica ed Applicata, 53, 331-345; doi:10.4430/bgta0049.

Westerhaus, M., and W. Welle (2002). Environmental effects on tilt measurements at Merapi volcano, Bull. Inf. Marees Terr., 137, 10917-10926.

Wyatt, F.K., S.-T. Morrissey and D.C. Agnew (1988). Shallow borehole tilt: A reprise, J. Geophys. Res., 93, 9197-9201.

Zadro, M., and C. Braitenberg (1999). Measurements and interpretations of tilt-strain gauges in seismically active areas, Earth Science Reviews, 47, 151-187.

*Corresponding author: Ciro Ricco,
Istituto Nazionale di Geofisica e Vulcanologia, Sezione di Napoli, Osservatorio Vesuviano, Naples, Italy;
email: ciro.ricco@ov.ingv.it.